



Experimental and numerical analyses for designing two-pot biomass cookstove

Rohan R. Pande¹ · Sanjay K. Sharma² · Vilas R. Kalamkar³

Received: 20 January 2019 / Accepted: 20 July 2019 / Published online: 2 August 2019
© The Brazilian Society of Mechanical Sciences and Engineering 2019

Abstract

The use of cookstoves is as old as human civilization, and food cooking is considered to be one of the major steps responsible for human brain development. Around 60% of the world population still relies on the use of biomass cookstoves for cooking and heating needs. The present work is an attempt to find a better and easy solution for designing a cookstove. A mathematical approach is presented in the paper to determine the performance of a cookstove to reduce the trial and error method of experimentation. The mathematical model is verified and validated with the experimental results. Three sets of water boiling test are performed to measure the cookstove performance. The average deviation in the model predicted and the experimental values for mass flow rate, temperature and thermal efficiency is 4.4%, 9%, and 7%, respectively. To determine the exhaust values, the mathematical outputs are set as the computational model input and the values of temperature, exhaust and flow structures are determined. The exhaust values of the computational model are in good agreement with the experimental results.

Keywords Cookstove · Modelling · Water boiling test · Computational fluid dynamics

1 Introduction

The biomass cookstove usage is as old as human civilization. Majority of the world population (55%) lives in rural areas, and this situation will remain until 2050 [1] who depend primarily on biomass. Even today, the biomass cookstove is the first choice of rural people in many developing countries. India is one such country, where 70% of its population still lives in rural areas and about 66% and 32% of its rural and

urban population still depend on traditional biomass, as a source of total primary energy need, as per the report of Ministry of renewable energy (MNRE), India. The traditional biomass cookstoves suffered with inefficient design and more emissions, causing environmental and health hazard issues. Modernization of the biomass cookstoves, in India, started in the 1940s in terms of cookstove design, alternative fuel used and to reduce indoor air pollution (IAP) [2]. The first improved model of biomass cookstove developed in the late 1940s was Magan Chulha, reported in the literature. However, the success was limited in terms of performance and efficiency. During the 1950s, the initiative was taken by the western countries in developing the improved biomass cookstoves for the rural people of third world country [3]. The oil crisis during 1970 also helped in generating the wave for improvement in biomass cookstoves. It also dragged the total attention towards environmental issues and conservation measures associated with biomass cookstoves. The scientific progress in the design of biomass cookstove started in the 1980s. Figures 1 and 2 show the progress in the field of biomass cookstove in terms of research papers published year-wise and country-wise, respectively [4]. In the present time, a wide variety of developed cookstoves are available for usage by the locals in the different parts

Technical Editor: Mário Eduardo Santos Martins.

Electronic supplementary material The online version of this article (<https://doi.org/10.1007/s40430-019-1839-z>) contains supplementary material, which is available to authorized users.

✉ Vilas R. Kalamkar
rohanpande1991@yahoo.com;
vilas.kalamkar@rediffmail.com

- ¹ Department of Mechanical Engineering, G H Raisoni College of Engineering, Nagpur, India
- ² School of Mechanical Engineering, Lovely Professional University, Phagwara, Punjab, India
- ³ Visvesvaraya National Institute of Technology, Nagpur 440010, India

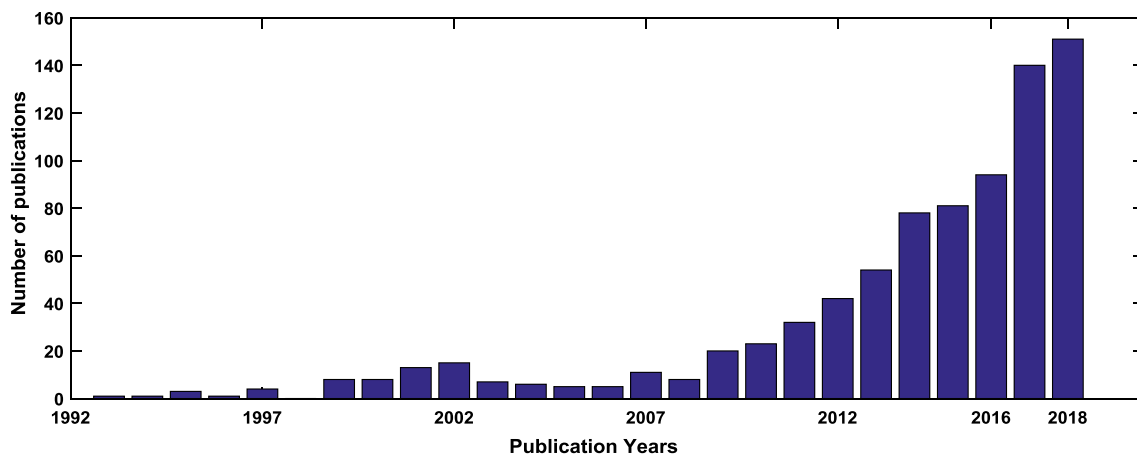


Fig. 1 Publication with years worldwide Source: Web of science

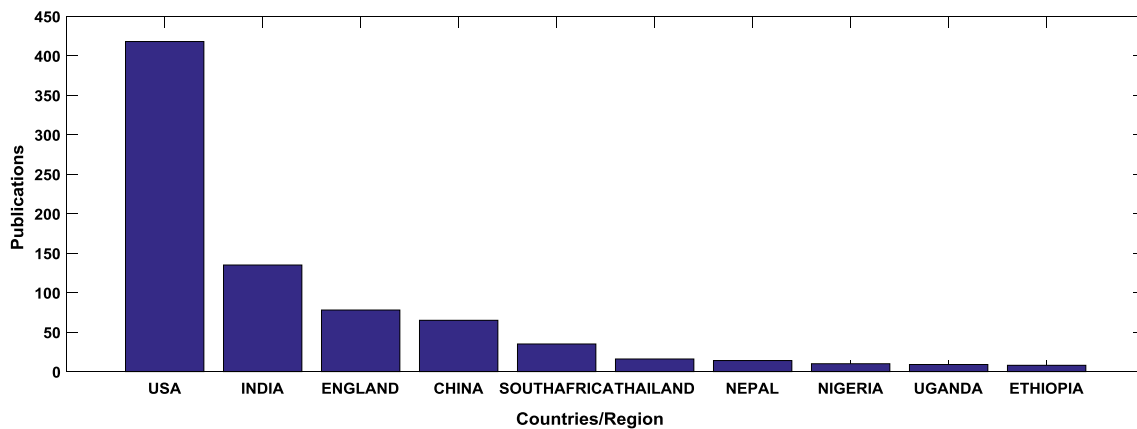


Fig. 2 Country-wise publications Source: Web of science

of the world [5–10]. India launched the first programme on improved Chulhas (or biomass cookstoves), National programme on improved Chulha (NPIC) during 1985–86 [11]. Baldwin [5] introduced general semi-empirical guidelines to design and improve the performance of cookstove. In 1954, the first laboratory test was conducted by Theodorovic in Egypt. The design aspects of the stove were shifted to the monitoring of exhaust coming out of the stove for measuring its performance during the early 1980s. The various methods were used to measure the performance parameters of the stove. Different testing protocols for the working of cookstove were also developed. The testing methods help to compare different stoves (Chulhas), considering various parameters. In 1980, Intermediate Technology Development Group (ITDG) came up with the procedure for testing of a cookstove in the laboratory as well as in the field [11]. Subsequently, in 1982 Volunteers in Technical Assistance (VITA) carried out further work on the above to release a

draft protocol as a provisional international standard [12]. These standard procedures were reviewed and accepted in 1985 by several groups working on cookstoves. Therefore, the three testing protocols, namely water boiling test (WBT), kitchen performance test (KPT) and controlled cooking test (CCT), are the most popular testing methods used by the researchers. In 1991, Bureau of Indian Standards (BIS) adopted the water boiling test as its own standard to test the biomass cookstoves, which also included the measurement of CO/CO₂ ratio as a separate test. The summary of different testing protocols is well explained in research articles [7, 8].

The current investigations are mostly focused on the reduction of pollutants coming out from the traditional cookstoves by introducing the “improved single-pot” cookstoves [13–16]. Many parameters, influencing the performance of cookstoves, were identified and studied by researchers [17–26]. The effect of moisture content [21, 22], different types of fuels [21, 23, 24] and different design aspects [5, 25,

[26] are investigated. Few researchers [27, 28, 30] also conducted the field surveys and evaluation of many improved “single-pot” cookstoves. However, the majority of work so far deals with the single-pot cookstoves, and very few work has been reported on “multipot” natural draft biomass cookstoves. Most of the houses in rural areas in India use a multipot biomass cookstove [29].

The recent research on the performance investigations with the experiment on the multipot cookstoves lack geometrical design parameters consideration. Moreover, these experiments were conducted on a trial and error basis. Till date, no contemporary research provides a mathematical model on the multipot cookstove. There are few investigations on the multipot cookstove: Oanh et al. [22], in his research work, presented the results of 12 selected wood-burning cookstove used in Asia. Out of the 12, metallic and ceramic made Nepalese 2-pots were the multipot cookstoves used. The overall performance of the stove was poor with thermal efficiency lower than 20%. The emission of particulate matter and polyaromatic hydrocarbon was highest among the other stoves. Bhattacharya et al. [26] compared the emission of the Nepalese cookstoves used by Oanh [22] with wood and charcoal. The thermal efficiencies were below 15%, and the emission factors were also not appreciable. The emission factors for ceramic and metallic pot cookstoves were around 113 and 45 g/kg of fuel used, respectively. Honkalaskar et al. [30] performed experiments on two-pot and three-pot cookstoves by inserting the twisted tape device. The experimental results showed a substantial decrease in the fuel consumption and soot accumulation. Also, the cooking time was reduced by around 18.5%. However, the making of twisted tape is not an easy task for the local artisans/blacksmith; it involves cutting, drilling, heating, twisting and welding operations. Though the authors claim to show some improvement in the performance of cookstove, no detailed analysis was presented in the paper. Joshi and Srivastava [31] performed experiments on three-pot cookstove and compared the results with the traditional mud stove. The paper failed to present the detailed analysis of WBT results. MaCarty et al. [32] presented the results of fifty cooking stoves in the laboratory, and few of the stoves were multipot cookstove. They used two-pot cookstoves like Uganda 2-pot cookstove, Onil stove and Justa stove along with the other stoves. All the stoves were provided with the chimney and used sunken pots. The efficiencies for Onil and Justa stoves are below 25% with the highest fuel consumption, among the fifty cookstoves. The highest efficiency of 35% was obtained with Uganda 2-pot; however, the diameter of the vessel used for operation was less than that of the cookstove hole, restricting the users to use specific vessels for the stove. The chimney also needed continuous monitoring to keep the “indoor air” pollutants free.

2 Need of study

The use of firewood in rural areas is still predominant, since it is often the only acceptable, accessible and affordable fuel in the region. Acceptability of firewood is very high since ancient times and has therefore shaped cooking habits accordingly. Accessibility of firewood is a crucial factor as it is available closely to their homestead for cooking purpose, especially in rural areas where LPG is not easily available. Also, the biomass is available year-round and not susceptible to heavy seasonal fluctuations. Affordability plays a decisive role in the use of firewood for cooking, as many households can collect firewood for free, so it remains the cheapest energy source for cooking and heating. However, it must be recognized that firewood would be extremely expensive if the additional cost of labour done by women and children collecting firewood were considered and the negative impacts on health and the environment are internalized.

Around 3–4 million people prematurely die every year, and many more are affected by morbidity due to indoor air pollution (IAP). Speaking about India, the reports from the India State-Level Disease Burden Initiative report 2017 [34], around 12.4 lakh deaths occurred due to air pollution, out of which 4.8 lakh deaths were attributed to IAP. The root cause for IAP is the exhaust coming out of the traditional biomass stoves. The toxic gases like carbon monoxide, polycyclic aromatic hydrocarbons and soot particles contribute to IAP [23, 33–35]. The health-damaging carbon monoxide and particulate matter cause chronic obstructive lung disease, respiratory infections and many such fatal diseases [36]. According to a World Health Organization report [37], smoke from biomass cookstove inhaled by the operator is equivalent to smoking 400 cigarettes in an hour and causes severe respiratory and other diseases. Out of the million deaths globally, 27% are due to pneumonia, 18% from stroke, 27% from ischemic heart disease, 20% from chronic obstructive pulmonary disease (COPD), and 8% from lung cancer. Majority of the deaths occur among the person handling (who happen to be females) the cookstove, and hence, awareness programmes regarding the adverse effect of IAP should be conducted. In spite of such fatal consequences, people have not stopped using cookstoves, especially in rural areas. However, in urban areas, firewood for cooking has been dominantly replaced by LPG or other modern fuels [38, 39]. The main reason is the free availability of fuel and the least maintenance cost of cookstoves. Every house in a rural place uses a single- or multipot biomass cookstove.

The use of biomass cookstove has also contributed to deforestation over past years in developing countries. The fuel consumption is high due to very low thermal efficiency of traditional biomass cookstove. So it is very necessary to know the dependency of different parameters to enhance

the thermal performance of the cookstove. The major hindrance is the measurement of the performance on the field, as the result differ quickly. Therefore, a mathematical model is proposed to save time and energy resource. Hence, the present work is an attempt to minimize the efforts required for the experimentation process and avoid the costly instruments to predict the performance of the cookstove. The work comprises mathematical modelling, experimentation and computational approach to determine the performance of cookstoves.

2.1 Methodology

2.1.1 Mathematical model

The modified geometry is selected from the two-pot cookstoves used in the rural parts of Maharashtra by doing the survey [29]. The model geometry consists of a single feeding zone, a primary combustion chamber and a secondary zone where second pot can be placed.

The model is shown in Fig. 3. The cookstove is divided into different zones as shown in Fig. 3.

- Zone 1: a primary zone where the combustion takes place
- Zone 2: an intermediate zone which connects zone 1 and zone 3
- Zone 3: a secondary zone where flame from zone 1 propagates
- Zone 4: pot 2 bottom
- Zone 5: pot 2 gap
- Zone 6: sides of pot 2

2.1.2 Assumptions

The cookstove involves a complex combustion phenomena. The heat transfer occurs through conduction, convection and radiation. To simplify such complex phenomena, certain assumptions were made without neglecting the important aspects of cookstove operation. The assumptions are as follows:

1. The temperature and the emissivity of burning char are taken as 1100 K and 0.85, respectively [20, 40–42].
2. The emissivity of the stove inner surface and pot bottom is 1. (The few trials before the final reading turn both the surfaces black due to soot deposition).
3. The pressure drop across the combustion bed is negligible.
4. There is no pot gap between zone 1 and pot 1; hence, the mass of flue will remain constant throughout all the zones till exit.

The correlations used to model the two-pot cookstove are as follows:

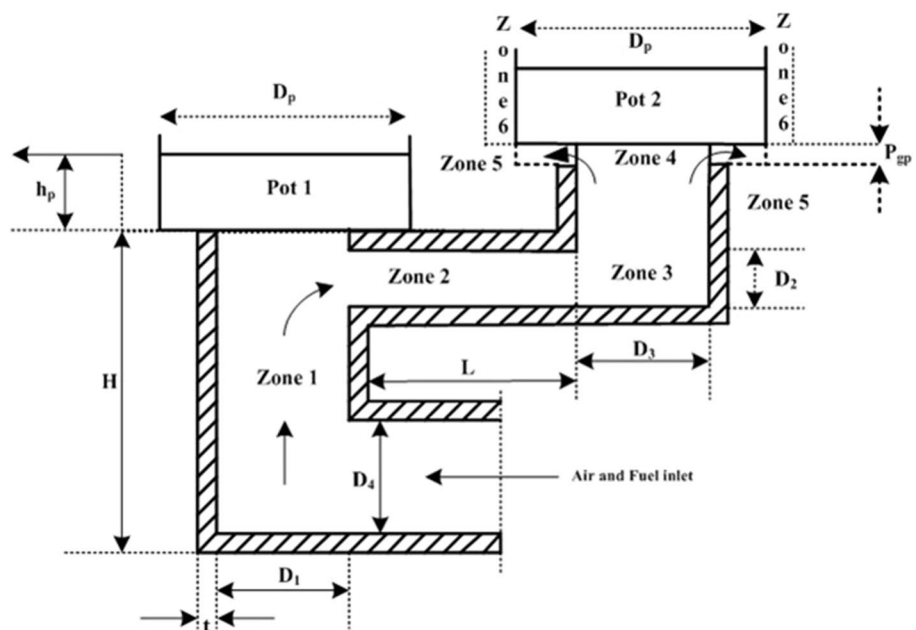
$$\mu = 0.3501 \times T^{0.69} \times 10^{-6} \tag{1}$$

$$k = 8 \times 10^{-5} \times T^{1.0152} \tag{2}$$

$$\rho = \frac{359.7}{T^{1.003}} \tag{3}$$

$$C_p = 415.6 \times T^{0.1591} \tag{4}$$

Fig. 3 Modified two-pot cookstove model



$$g = 0.0009 \times T^{1.7097} \times 10^{-6} \tag{5}$$

$$h_s = 0.00032273 \times T^2 + 1.64833661388 \times T + 2021.531847 \tag{6}$$

2.1.3 Mathematical equations

Zone 1

Combustion chamber

The fuel combustion takes place in this zone. It is the feeding zone, through which the fuel input is metered. Thus, the amount of air entering is controlled by changing the inlet area ratio (IAR) [20]. The losses like char radiation, flame radiation, heat losses through the walls and feed door (inlet opening) are taken into consideration. In addition, sensible heat loss of hydrogen and moisture present in fuel are substantial and are included in the modelling.

$$IAR = \frac{\text{Area unoccupied by the feed door}}{\text{cross - sectional area of the chimney}} \tag{7}$$

Applying heat balance for Zone 1,

$$Q_1 = Q_2 - (Q_3 + Q_4 + Q_5 + Q_6 + Q_7 + Q_8) \tag{8}$$

where

Q_1 is the heat gain by the flue gases and Q_2 is the actual amount of heat supplied by the fuel, while Q_3, Q_4, Q_5, Q_6, Q_7 and Q_8 are different heat transfer losses in zone 1 as shown in Fig. 4.

$$Q_1 = m_{\text{actual}} \times C_{p,fg1} \times (T_{fg1} - T_{\text{amb}}) \tag{9}$$

$$m_{\text{actual}} = C_d \times \frac{359.7}{T_{fg1}^{1.003}} \times A_{\text{cross}} \sqrt{2 \times g \times (H' - D_2 - t) \left(\frac{T_{fg1}}{T_{\text{amb}}} - 1 \right)} \tag{10}$$

C_d is the coefficient of discharge which accounts for losses occurring in the cookstove due to viscous effects and flow distribution of combustion process. The value of C_d varies from 0 to 1 for the different types of chimneys [17, 43, 44]

$$Q_2 = \dot{m}_f \times \text{NCV} \tag{11}$$

$$\dot{m}_f = \frac{\text{FP}}{\text{NCV}} \tag{12}$$

Using the radiation network method [45], char bed radiative heat transfer and flame radiative heat transfer (Q_3 and Q_4) are given as:

$$Q_3 = \frac{\sigma \times A_{\text{cross}} \times (T_{\text{char}}^4 - T_{p1}^4)}{\frac{1-\epsilon_c}{\epsilon_c} + \frac{2}{1+F_{c-p}}} \tag{13}$$

$$Q_4 = \sigma A_1 (\epsilon_1 T_{fg1}^4 - \alpha_1 T_{p1}^4) \tag{14}$$

The standard expressions for emissivity and absorptivity in terms of temperature [46] are given as,

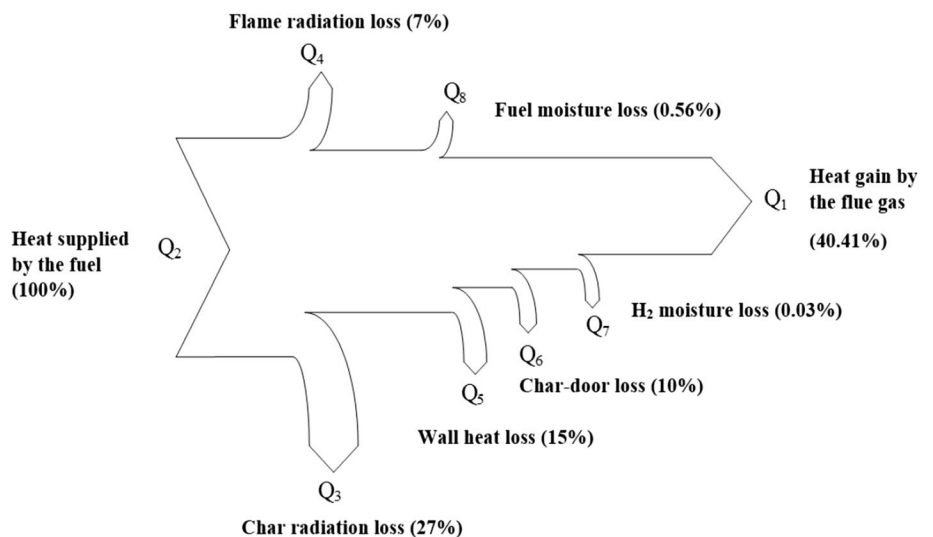
$$\epsilon_1 = e^{A+B \ln \left(0.2 * 3.6 \frac{V_{pm}}{A_{pm}} \right)} \tag{15}$$

$$\alpha_1 = \epsilon_1 \times \left(\frac{T_{fg}}{T_s} \right)^{0.5} \tag{16}$$

$$A = 0.848 + 9.02 \times 10^{-4} T_{fg1} \tag{17}$$

$$B = 0.9589 + 4.8 \times 10^{-6} T_{fg1} \tag{18}$$

Fig. 4 Sankey diagram for heat balance (for FP—3.119 kW)



where

$$V_{pm} = \frac{\pi}{4} \times D_1^2 H' \tag{19}$$

$$A_{pm} = \frac{\pi}{4} \times D_1^2 \tag{20}$$

The heat loss from flame to outer surrounding in zone 1 is given as,

$$Q_5 = \frac{T_{fg1} - T_{amb}}{\frac{1}{(h_{ci1} + h_{fr1} + h_{rch1})A_{r1}} + \frac{\ln\left(\frac{D_{o1}}{D_1}\right)}{2\pi H'_1 K_{insu}} + \frac{1}{(h_{co1} + h_{ro1})A_{o1}}} \tag{21}$$

The convective heat transfer coefficient of inside combustion chamber is estimated using the Dittus–Boelter equation as given as [47]:

$$h_{ci1} = \frac{k_1}{D_1} \times 0.023 \times Re_{D_1}^{0.8} \times Pr^{0.4} \tag{22}$$

The convective heat transfer coefficient for an outer wall is derived for all values of $Gr \times Pr$, considering constant heat flux.

$$h_{co1} = \frac{k_{flue\ gas}}{H'_1} \times \left[0.825 + \frac{0.387(Gr \times Pr)^{0.167}}{\left\{ 1 + \left[\frac{0.437}{Pr} \right]^{0.5625} \right\}^{0.296}} \right] \tag{23}$$

$$h_{ro1} = \sigma \epsilon_2 (T_{wo1}^2 + T_{amb}^2) (T_{wo1} + T_{amb}) \tag{24}$$

$$h_{fr1} = \frac{\sigma (\epsilon_1 T_{fg1}^4 - \alpha_1 T_{wi1}^4)}{T_{fg1} - T_{wi1}} \tag{25}$$

$$h_{chr} = \frac{\sigma (T_{char}^2 + T_{wi1}^2) \times (T_{char} + T_{wi1})}{\frac{1-f_c}{\epsilon_c} + \frac{F_{c-w} + F_{c-p}}{F_{c-w}(F_{c-w} + 2 \times F_{c-p})}} \tag{26}$$

The shape factor [46] and configuration factors [48, 49] are calculated using

$$F_{c-p} = \frac{\left(D_1^2 + 2(H'_1 + W_{i1})^2 - 2(H'_1 + W_{i1})\sqrt{D_1^2 + (H'_1 + W_{i1})^2} \right)}{D_1^2} \tag{27}$$

$$F_{c-w} = 1 - F_{c-p} - F_{c-d} \tag{28}$$

The losses of energy in feeding zone, i.e. from the combustion chamber bed to feeding door, are as follows:

$$Q_6 = F_{c-d} \times \sigma \times A_{cross} \times \left((T_{char})^4 - (T_{amb})^4 \right) \tag{29}$$

$$Q_7 = (h_s - 2547) * 0.09 * H_2 * \dot{m}_f \times 1000 \tag{30}$$

$$Q_8 = \left(h_s - 4.187 \times (T_{amb} - 273) \times \left(\frac{M}{100 - M} \right) \times \dot{m}_f \right) \times 1000 \tag{31}$$

Also,

Heat transfer from the flame to inner wall = heat transfer from inner wall to outer wall = heat transfer from outer wall to the surrounding,

$$Q_9 = \frac{(T_{fg1} - T_{wi1})}{\frac{1}{(h_{ci1} + h_{fr1} + h_{chr}) \times A_{r1}}} = Q_{10} = \frac{(T_{wi1} - T_{wo1})}{\frac{\ln\left(\frac{D_{o1}}{D_1}\right)}{2\pi \times H'_1 \times K_{ins}}} = \tag{32}$$

$$Q_{11} = \frac{(T_{wo1} - T_{amb})}{\frac{1}{(h_{co1} + h_{ro1}) \times A_{o1}}}$$

Solving Eq. (8) and Eq. (32), we get the values of T_{fg1} , T_{wi1} and T_{wo1} .

Zone 2

The flue gas temperature in zone 2 (T_{fg2}) is estimated by averaging the temperature $T_{central1}$ at the entrance of the zone 2 and $T_{central2}$ at the exit. The equations used to determine the value of $T_{central1}$ are as follows:

$$Q_{pot1} = (h_{conv} + h_{rad}) \times A_{pot1} \times \left(\frac{T_{fg1} + T_{central1}}{2} - T_{p1} \right) \tag{33}$$

$$h_{rad} = \epsilon_1 \times \sigma \left(\frac{T_{fg1} + T_{central1}}{2} + T_{wi} \right) \left(\left(\frac{T_{fg1} + T_{central1}}{2} \right)^2 + T_{wi}^2 \right) \tag{34}$$

$$Q_1 - Q_{pot1} = m_{actual} \times C_{p\ fg2} \times (T_{central1} - T_{amb}) \tag{35}$$

The equations used to determine the value of $T_{central2}$ are as follows:

$$m_{actual} \times C_{p\ fg1-2} (T_{central1} - T_{amb}) - Q_{12} = m_{actual} \times C_{p\ fg2-3} (T_{central2} - T_{amb}) \tag{36}$$

$$Q_{12} = \frac{T_{central} - T_{amb}}{\frac{1}{(h_{ci2} + h_{fr2})A_{r2}} + \frac{\ln\left(\frac{D_{o2}}{D_2}\right)}{2\pi H'_2 K_{insu}} + \frac{1}{(h_{co2} + h_{ro2})A_{o2}}} \tag{37}$$

The convective heat transfer coefficient for the inner flame in zone 2 is given as:

$$h_{ci2} = \frac{k_{flue\ gas}}{L} \times \left[4.82 + 0.0185 \times (Re_D \times Pr)^{0.827} \right] \tag{38}$$

$$h_{ro2} = \sigma \epsilon_5 \left((T_{wo1})^2 + (T_{amb})^2 \right) (T_{wo1} + T_{amb}) \tag{39}$$

$$h_{co2} = \frac{k_{\text{flue gas}}}{L} \times \left\{ 0.6 + 0.387 \left[\frac{Gr_{D2} \times Pr}{\left\{ 1 + \left(\frac{0.559}{Pr} \right)^{0.5625} \right\}^{0.296}} \right]^{0.167} \right\}^2 \tag{40}$$

The convective heat transfer coefficient (h_{co2}) for an outer wall is obtained at film temperature.

Again, from the analogy of multimode heat transfer for the wall in zone 2, we have,

$$Q_{13} = \frac{T_{\text{central}} - T_{wi2}}{\frac{1}{(h_{ci2} + h_{rf2}) \times A_{i2}}} = Q_{14} = \frac{T_{wi2} - T_{wo2}}{\frac{\ln \left(\frac{D_{o2}}{D_{i2}} \right)}{2 \times \pi \times L \times K_{ins}}} \tag{41}$$

$$Q_{15} = \frac{T_{wo2} - T_{\text{amb}}}{\frac{1}{(h_{co2} + h_{ro2}) \times A_{o2}}} = Q_{12}$$

$$T_{\text{central}} = \frac{T_{\text{central}1} + T_{\text{central}2}}{2} = T_{fg2} \tag{42}$$

Solving Eqs. (35), (36) and (41), we get $T_{\text{central}2}$, T_{wi2} and T_{wo2} .

Zone 3 and zone 4 (pot 2)

The different heat zones for pot 2 have been solved for the various parameters using the heat balance equations

$$\begin{aligned} & m_{\text{actual}} \times C_{p4} \times (T_{\text{central}2} - T_{\text{amb}}) - Q_{16-27} \\ & - (m_{\text{actual}} \times C_{p5} \times (T_{e3} - T_{\text{amb}})) \\ & - Q_{\text{pot}2} = m_{\text{actual}} \times c_p (T_{e3} - T_{\text{amb}}) \end{aligned} \tag{43}$$

The heat loss from the wall of stove body in zone 3 of pot 2 is given as

$$Q_{16} = \frac{T_{fg3} - T_{\text{amb}}}{\frac{1}{(h_{ci3} + h_{fr3})A_{i3}} + \frac{\ln \left(\frac{D_{o3}}{D_{i3}} \right)}{2\pi H'_2 K_{insu}} + \frac{1}{(h_{co3} + h_{ro3})A_{o3}}} \tag{44}$$

The different heat transfer coefficients for pot 2 are determined in the similar fashion as that of pot 1

$$h_{ci3} = \frac{k_{\text{flue gas}}}{D_3} \times 0.023 \times Re_{D_1}^{0.8} \times Pr^{0.4} \tag{45}$$

$$h_{co3} = \frac{k_{\text{flue gas}}}{(D_2 + 2 \times t)} \times \left[0.825 + \frac{0.387(Gr \times Pr)^{0.167}}{\left\{ 1 + \left[\frac{0.437}{Pr} \right]^{0.5625} \right\}^{0.296}} \right] \tag{46}$$

$$h_{ro3} = \sigma \times \epsilon_6 \times (T_{wo3}^2 + T_{\text{amb}}^2)(T_{wo3} + T_{\text{amb}}) \tag{47}$$

Using the multimode heat transfer through walls of zone 3, we have,

$$Q_{17} = \frac{T_{fg3} - T_{wi3}}{\frac{1}{(h_{ci3} + h_{fr3})A_{i3}}} = Q_{18} = \frac{T_{wi3} - T_{wo3}}{\frac{\ln \left(\frac{D_{o3}}{D_{i3}} \right)}{2\pi \times (D_2 + t) \times K_{ins}}} \tag{48}$$

$$Q_{19} = \frac{T_{wo3} - T_{\text{amb}}}{\frac{1}{(h_{co3} + h_{ro3})A_{o3}}} = Q_{16}$$

$$Q_{\text{pot}2} = (h_{\text{conv}3} + h_{\text{rad}3}) \times A_{\text{pg}1} \times \left(\frac{T_{fg3} + T_{e3}}{2} - T_{p2} \right) \tag{49}$$

$$h_{\text{conv}3} = \frac{k_{\text{bottom}}}{D_3} \times 0.726 \times Re_{D2}^{0.53} \times \left(\frac{W_i}{D_2} \right)^{-0.191} \tag{50}$$

$$h_{\text{rad}3} = \sigma \times \epsilon_7 \times \left(\frac{T_{fg3} + T_{e3}}{2} + T_{wi3} \right) \left[\left(\frac{T_{fg3} + T_{e3}}{2} \right)^2 + (T_{wi3})^2 \right] \tag{51}$$

The change in enthalpy of flue gas leaving zone 3 is,

$$Q_{20} = m_{\text{actual}} \times (h_{fg3} - h_{e3}) \times 1000 \tag{52}$$

The heat gain by flue gases leaving zone 3 is taken by pot bottom,

$$Q_{21} = h_{\text{conv}3} \times A_3 \times \left(\frac{T_{fg3} + T_{e3}}{2} - T_{p2} \right) \tag{53}$$

Solving the above equations, we can get the values of T_{e3} and T_{fg3} , T_{wi3} , T_{wo3}

Zone 5 (for pot 2)

Pot 2 gap

The heat transfer on pot bottom surface using heat balance is given as

$$Q_{22} = m_{\text{actual}} \times (h_{e3} - h_{c3}) \times 1000 \tag{54}$$

$$\begin{aligned} Q_{23} &= h_{\text{pot gap}} A_{\text{pg}} \times \left(\frac{T_{c3} + T_{e3}}{2} - T_{p2} \right) + \sigma \times A_{\text{pg}} \\ &\times \left(\epsilon_8 \left(\frac{T_{c3} + T_{e3}}{2} \right)^4 - \alpha_4 (T_{p2})^4 \right) \end{aligned} \tag{55}$$

And, the heat transfer coefficient is evaluated by,

$$h_{\text{pot gap}} = \frac{k_{\text{pg}}}{D_3} \times 0.726 \times Re_{D2}^{0.53} \times \left(\frac{W_i}{D_3} \right)^{-0.191} \tag{56}$$

Solving Eqs. (54) and (55), we get T_{c3}

Pot 2 side (zone 6)

The convective and radiative heat transfer from flue gas coming out through zone 3 increases efficiency of the cookstove. The heat losses from the sides of the pot to the surroundings are also considered in this zone.

The convective and the radiative heat transfer in this zone is calculated using the following equations

$$Q_{24} = h_{\text{side}3} \times A_{\text{side}1} \times \left(\frac{T_{c3} + T_{o3}}{2} - T_{p2} \right) \quad (57)$$

$$Q_{25} = \sigma \times A_{\text{side}1} + \left\{ \varepsilon_9 \left(\frac{T_{c3} + T_{o3}}{2} \right)^4 - \alpha_5 \times T_{p2}^4 \right\} \quad (58)$$

The heat loss from pot side to the surrounding is calculated by assuming the combined convective and radiative heat transfer coefficient to be $10 \text{ W/m}^2\text{K}$.

$$Q_{\text{side loss}} = 10 \times A_{\text{side}1} \times \left(\frac{T_{c3} + T_{o3}}{2} - T_{\text{amb}} \right) \quad (59)$$

$$h_{\text{side}} = \frac{k_{\text{side}}}{h_w} \times 0.664 \times (Re_{\text{hw}})^{0.5} \times Pr^{0.333} \quad (60)$$

$$Q_{27} = m_{\text{actual}} \times (h_{c3} - h_{o3}) \times 1000 \quad (61)$$

$$Q_{26} = Q_{24} + Q_{25} + Q_{\text{side loss}} \quad (62)$$

Solving Eq. (62) gives T_{o3}

Thus, the overall efficiency can be calculated as,

$$\eta_o = \frac{Q_{\text{pot}1} + Q_{\text{pot}2} + Q_{24} + Q_{25} + 0.67Q_3}{FP} \times 100 \quad (63)$$

2.2 Performance evaluation criterion

The geometrical parameters were selected by considering the thermal efficiency and excess air ratio (EAR). The values of thermal efficiency for natural draft biomass cookstove should be above 25% as per the MNRE, India. Also, as per the guidelines for evaluating the performance of cookstove given by international workshop agreement (ISO 2012), the stove is rated between five-tiered (0–5) rating system for fuel use and emissions. For the stove to lie above Tier 2, the efficiency of the stove should be greater than 25%. Since the model fails to present the exhaust, an indirect method of the evaluation of combustion is applied. As excess air has some advantages and disadvantages, it should have some safe limit. Excess air increases the turbulence and promotes mixing in the combustion chamber ensuring complete fuel combustion. It converts the harmful gases of CO into CO₂. It also lowers the formation of unburned hydrocarbons. However, the excess air reduces the thermal efficiency and combustion temperature and increases the value of NO_x. Hence, there has to be some limit for the value of EAR.

Hence, there has to be some limit of excess air ratio (EAR). Prasad et al. [50] suggested that the excess air factor should lie between 1.5 and 2.5 for safe working of stove. Liu et al. [51] claimed that the optimize value for EAR is 2. Hasen et al. [52] suggested the best wood combustion occurs when the value ranges between 1.4 and 1.6. Carvalho et al. [53] recommended the EAR value of 1.6–2.2 for minimum CO emissions. Obaidullaha et al. [54] performed experiments on wood stove with capacity 10 kW and 20 kW and found the EAR values of 1.76 and 2.05 for minimum CO emissions for the 10 kW and 20 kW, respectively. Kshirsagar and Kalamkar [34] suggested the region of good combustion which is bounded by limiting value of the excess air ratio between 1.95 and 5.98. Ingwald et al. [55] claimed that for gas burner the excess air factor is around 1.2 for almost complete gas burnout regarding CO and organic compounds. Jian Sun et al. [56] performed experimentation on wood-burning stove and measured the value of exhaust. It was found that the optimized EAR is 2.5. Hence, considering the above literature, the limiting value of EAR was set to be between 1 and 6 for safe working of stove.

2.3 Experimental method

The experimental set-up is shown in Fig. 5. The insulation was provided with ceramic wool to prevent the heat losses. Babool wood was used as fuel. The recorded quantities were mass of fuel required to boil water from pot 1, water temperature in both the pots, velocity of flue, time taken to boil, amount of char left and exhaust emissions, i.e. CO, CO₂, O₂ and particulate matter (PM). Table 1 shows the specifications of the instrument used. The duct with the cross section of $65 \times 65 \text{ cm}^2$ was used to collect the exhaust gas. An exhaust fan was connected at the end of the duct, and the velocity of the fan was controlled by a dimmer. The anemometer probe was placed exactly at the centre of the duct. Care was taken to control the velocity such that the combustion flame should not get disturbed. The probe for measuring the PM and a K-type thermocouple to measure the flue gas temperature was placed inside the hood. Thus, calculating the dilution

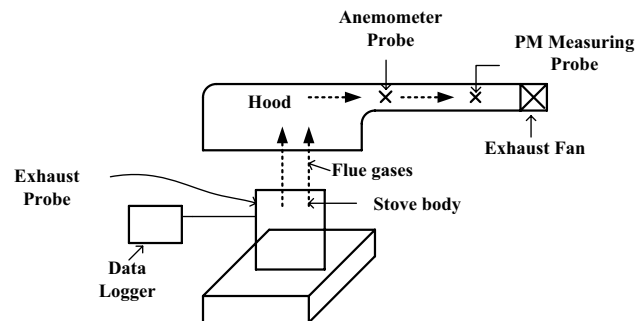


Fig. 5 Schematic of experimental set-up

Table 1 Instrumentation used in experimentation

Sr. no.	Instrument	Type/make	Range
1.	Flue gas analyser	Indus	CO: 0–1,000,000 ppm CO ₂ : 0–25% O ₂ : 0–25%
2.	Anemometer	Kanomax 6162	Temperature range of 500 °C
3.	Particulate measuring instrument	Air Veda	PM _{2.5} : 0–999 µg/m ³ PM ₁₀ : 0–1999 µg/m ³
4.	Weighing machine	LG electro	0–60 kg
5.	Exhaust fan 450 mm	Havells	1400 RPM

ratio the values of PM_{2.5} were obtained in µg/m³. The time taken to boil water from pot 1 was noted down by a stopwatch. The weight of the charcoal left was recorded to measure the exact dry fuel consumed. The firepower (FP) values obtained through three sets of water boiling test (WBT) were used as input for the proposed mathematical model. The flame temperature, thermal efficiency and exhaust obtained through the experimentation were compared with the mathematical model results.

2.4 Computational

The mathematical model has no provision to calculate the values of exhaust gases, and hence, using the mass flow rate of air from the mathematical model as an input to the computational model the exhaust coming out of the stove is calculated. Along with the exhaust values, the temperatures at different zones were calculated and validated with the experimental data. ANSYS Fluent 16.0 was used to simulate the combustion. The assumptions used are:

1. Since the average parameters over a length of operational time are more important, the operation of cookstove is assumed to be at steady state for a particular inlet area ratio and firepower [4, 46, 57–59].
2. A two-dimensional (2-D) model is considered for solving the computational domain to save the computational time [58, 60–62].
3. The exhaust generated in the domain does not undergo any further chemical change.

2.4.1 Grid independence test

It is important to have a grid independence test before solving any computational problem. It helps to save the computational time required to solve the given problem. Two temperature points T_1 and T_2 in the computational domain were monitored. Table 2 shows the independence test done for firepower 2.99 kW. The number of nodes was varied from 117,051 to 253,748. The values of T_1 and T_2 , at 170,410, 209,340 and 253,748 nodes were having the difference of

Table 2 Grid independence test

Sr. no.	No. of nodes	T_1	% Difference	T_2	% Difference
1.	11,7051	1080.76	–	846.13	–
2.	170,410	1035.12	–9.12	856.14	–1.18
3.	209,340	1041.35	0.96	861.42	–0.62
4.	253,748	1042.52	0.58	867.41	–0.70

less < 1%, so the simulation was carried out with 209,340 nodes.

The computational domain with the boundary conditions is shown in Fig. 6. The values of mass flow rates for different firepowers are given in Table 3. The effect of radiative and convective heat transfer is taken into account though walls and pot bottoms of the cookstove. At the exit, the pressure outlet condition is given.

2.4.2 Governing equations

The continuity, momentum and energy equations were solved in the non-premixed combustion model. The combustion chemistry of fuel was solved by generating probability density function table (PDF). The transport equation for conserved scalar mixture fraction is taken from Biswas and Eswaran [63].

$$\frac{\partial \rho}{\partial t} + \nabla \cdot (\rho v) = 0 \quad (64)$$

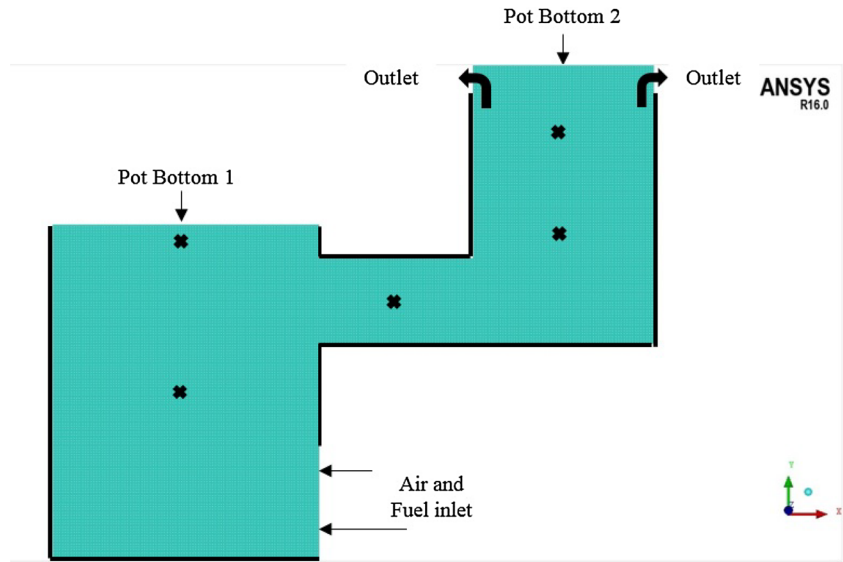
$$\frac{\partial (\rho v)}{\partial t} + \nabla \cdot (\rho v v) = -\nabla p - \nabla \tau + \rho g \quad (65)$$

In Eq. (2), the first and second right hand side terms are the pressure gradient and molecular transport due to viscosity, respectively, where τ is the viscous stress tensor.

$$\tau = -\mu \left[2S - \frac{2}{3} \nabla v \right] \quad (66)$$

$$S = \frac{1}{2} (\nabla v + \nabla v^T) \quad (67)$$

Fig. 6 Computational domain with the boundary conditions



*Thick lines in the figure presents the wall boundary condition

*Cross marks given in the figure are the positions of the R-type thermocouples

where ∇v^T is the transpose of the velocity gradient and μ is the dynamic viscosity

$$\frac{\partial(\rho H)}{\partial t} + \nabla \cdot (\rho v H) = \nabla \cdot \left(\frac{k_t}{C_p} \nabla H \right) + S_h \quad (68)$$

Equation (5) represents the energy equation.

where the total enthalpy H is defined as the sum of the mass fraction and enthalpy for the j th species.

$$H = \sum_j Y_j H_j \quad (69)$$

where H_j is defined as

$$H_j = \int_{T_{ref,j}}^T C_{p,j} dT + h_j^o(T_{ref,j}) \quad (70)$$

where $h_j^o(T_{ref,j})$ is the enthalpy of formation of species j at the j th reference temperature.

2.4.3 The PDF transport equation model

The non-premixed combustion probability density function (PDF) of the mixture fraction is selected for modelling the sub-grid scale mixing. The transport equation for conserved scalar mixture fraction is written as:

$$\begin{aligned} \frac{\partial(\rho P)}{\partial t} + \nabla \cdot (\rho v P) + (\rho g - \nabla \bar{p}) \cdot \nabla_v P + \sum_{i=1}^n \frac{\partial}{\partial \psi_i} [w_i P] \\ = \nabla_v \cdot [-\nabla \cdot \tau + \nabla(p' |v, \psi) P] - \sum_{i=1}^n \frac{\partial}{\partial \psi_i} [(\nabla \cdot (\rho D \nabla \psi_i) |v, \psi) P] \end{aligned} \quad (71)$$

The first two left hand side (LHS) terms of Eq. (71) are the local change and convection of the PDF in physical space. The third term represents transport in velocity space by gravity and the mean pressure gradient. The last term on the LHS contains the chemical source terms. In the right hand side (RHS) of the transport equation, there are two terms that contain gradients of quantities conditioned on the values of velocity and composition. Therefore, if gradients are not included as sample space variables in the PDF equation, these terms occur in unclosed form and have to be modelled. The first unclosed term on the RHS describes transport of the probability density function in velocity space induced by the viscous stresses and the fluctuating pressure gradient. The second term represents transport in reactive scalar space by molecular fluxes. This term represents molecular mixing. Many combustion simulations tend to ignore the effect of

Table 3 Mass flow rate at different firepowers

Sr. no.	Firepower (kW)	m_{fuel} (kg/s)	m_{air} experi- mental (kg/s)	m_{air} model predicted (kg/s)
1.	2.202	0.00013	0.0014	0.0013
2.	2.241	0.00014	0.0013	0.0012
3.	2.572	0.00016	0.0013	0.0012
4.	2.623	0.00016	0.0014	0.0012
5.	2.981	0.00018	0.0015	0.0012
6.	3.119	0.00018	0.0015	0.0013

Table 4 Temperatures at different zones

Sr. no.	Parameter	Description	Temperature (K)
<i>Zone 1</i>			
1.	T_{fg1}	Flame temperature in zone 1	1025
2.	T_{wi1}	Inner wall surface temperature for zone 1	1004
3.	T_{wo1}	Outer wall surface temperature in zone 1	593
<i>Zone 2</i>			
1.	$T_{central1}$	Temperature of flue-entering zone 2	784
2.	T_{wi2}	Inner wall surface temperature for zone 2	589
3.	T_{wo2}	Outer wall surface temperature of zone 2	446
4.	$T_{central2}$	Temperature of flue-leaving zone 2	769
	T_{fg2}	Average flame temperature in zone 2	
<i>Zone 3</i>			
1.	T_{fg3}	Flame temperature in zone 3	721
2.	T_{wi3}	Inner wall surface temperature in zone 3	549
3.	T_{wo3}	Outer wall surface temperature in zone 3	397
4.	T_{e3}	Temperature of flue-leaving zone 3	673
5.	T_{c3}	Temperature of flue at the corner of pot 2	649
6.	T_{o3}	Temperature of flue-leaving the side of pot 2	440

Table 5 Energy balance of the stove

	Energy encountered	Watt	%
1.	Charcoal bed radiative heat transfer	838.67	26.89
2.	Flame radiative heat transfer	216.49	6.94
3.	Heat loss due to hydrogen-related moisture in fuel	1.02	0.03
4.	Heat loss due to fuel moisture	17.33	0.56
5.	Heat loss in the feeding area	311.55	9.99
6.	Heat taken by pot 1 bottom	449.65	14.42
7.	Heat taken by pot 2 bottom	77.07	2.47
8.	Heat taken by side of the pots	34.11	1.09
9.	Heat loss through walls of different zones	604.60	19.39
10.	Heat lost to the exhaust flue	568.13	18.22
Total		3118.62	100.00

radiation in the calculations. This is because the governing radiative transfer equation is of integral–differential nature, which makes the analysis difficult and computationally expensive. The method and model selection was done by using ANSYS Fluent user manual guide.

3 Results and discussion

The equations were solved iteratively using a MATLAB® script, and the iterative solution yields 13 temperatures values. The other output parameters like mass flow rates, thermal efficiency, different heat encountered, enthalpies, etc., were then determined from these temperatures values and flue gas properties. The calculation for firepower (FP) = 3.119 kW for selected geometry is shown in Table 4.

The energy balance for the entire stove is given in Table 5.

Table 6 Average parameters of WBT test with standard deviations ($n = 3$)

Phase	Parameter	Unit	Value
High power	Thermal efficiency	%	26.74 ± 2.08
	Firepower	kW	2.60 ± 0.34
	Specific fuel consumption	g/l	89.25 ± 15.7
	Time taken to boil	Min	35.00 ± 10.18
	Dry fuel consumed	G	324.89 ± 60.31
	CO	g/MJ _d	10.59
	PM _{2.5}	mg/MJ _d	108.77
Lower power	Thermal efficiency	%	32.23 ± 2.36
	Firepower	kW	1.39 ± 0.17
	Specific fuel consumption	g/l	42.95 ± 5.47
	Turn-down ratio	–	1.80 ± 0.22

Three sets of WBT were performed on the model stove. The average performance parameters with standard deviations are given in Table 6 for high- and low-power phases. The parameters include thermal efficiency of the stove, specific fuel consumption, firepower, time taken to boil water, dry fuel consumed and the exhaust coming out of the stove. Few parameters like temperature, exhaust, mass flow rate are used to validate the mathematical and computational models. The relative error percentage which is the ratio of the difference between the experimental and model predicted to the experimental values was calculated using Eq. [64].

3.1 Flame temperature

The values of flame temperature were monitored by placing R-type thermocouple in each zone. Two thermocouples were

placed in the zone 1 and zone 3, while one more was placed in zone 2. The average temperatures in the zones were validated with the modelling results. Figures 7, 8 and 9 compare the variation of flame temperatures in different zones. The average temperature variations with the mathematical modelling for zone 1, zone 2 and zone 3 are 10%, 3% and 8%, respectively. Also, the average temperature variation with the computational modelling for zone 1, zone 2 and zone 3 is 7%, 12% and 13%, respectively. It can be seen that the values obtained through experimentation are less than those obtained through modelling. The possible reasons can be due to the placement of the thermocouples, due to the non-uniformity of flame temperatures in the radial directions, the assumption of a 2-D model and unaccounted losses.

Mass flow rate: The variation of mass flow rate of air with firepower is shown in Fig. 10. The model-predicted

Fig. 7 Variation of flame temperature in zone 1 with firepower

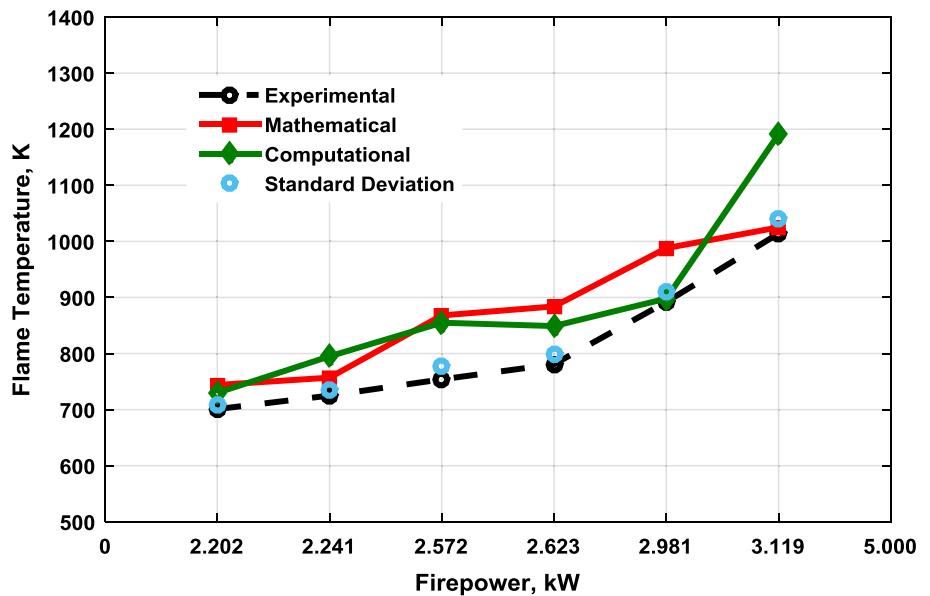


Fig. 8 Variation of flame temperature in zone 2 with firepower

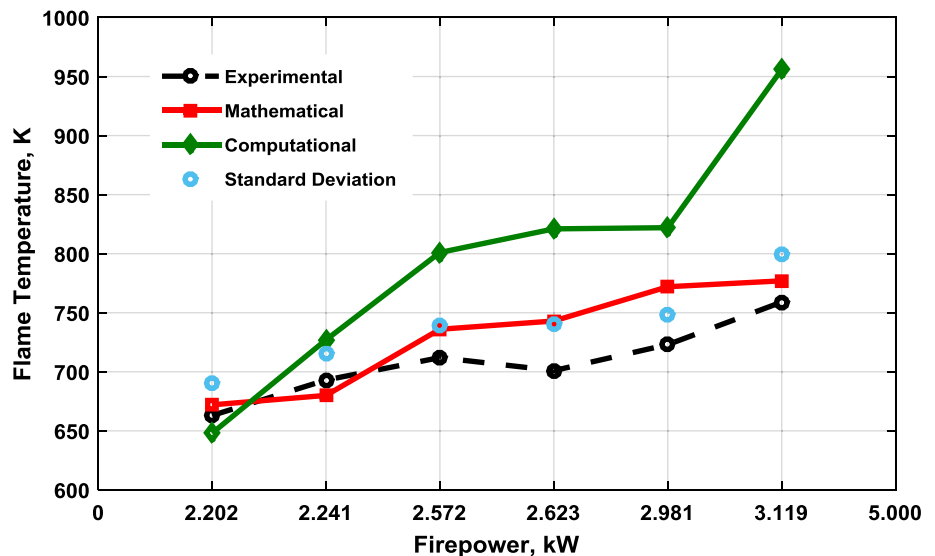


Fig. 9 Variation of flame temperature in zone 3 with firepower

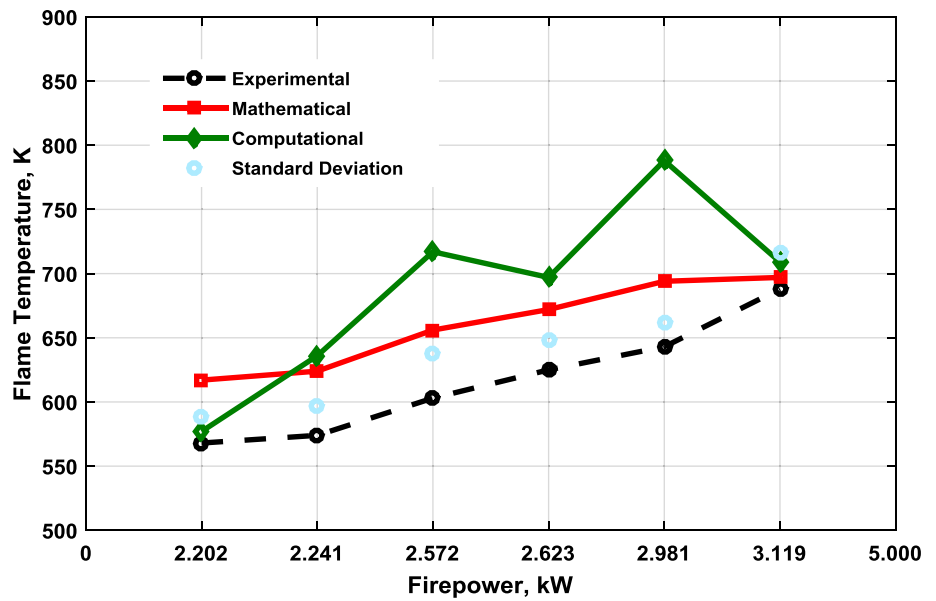
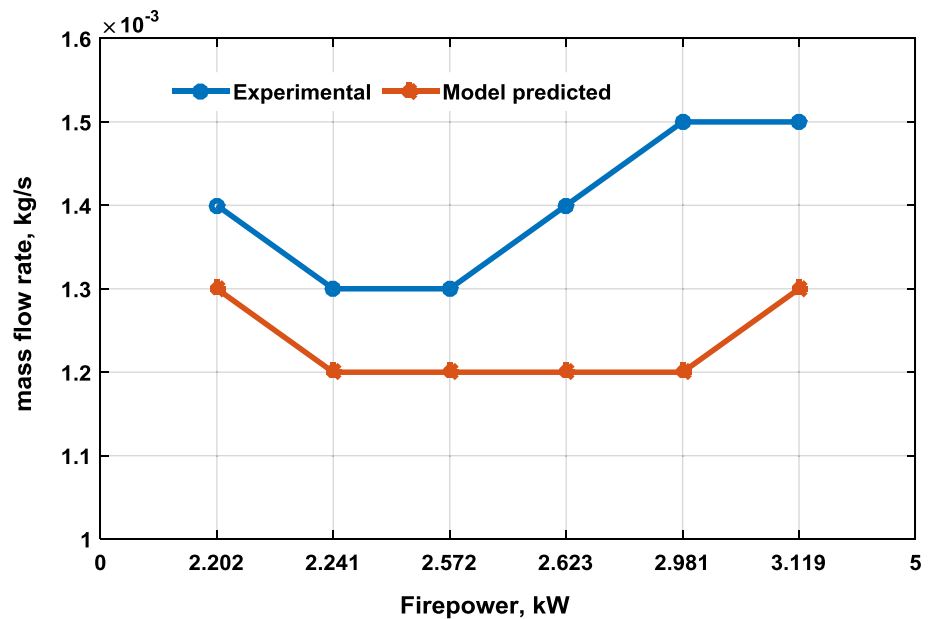


Fig. 10 Variation of mass flow rate with firepower



values are in good agreement with the experimental values. The average deviation is $\pm 10.88\%$. Six different values of firepower of hot start test are used to validate the mathematical model. The values of the air flow rate are calculated considering all the losses involved in the stove. Losses like fuel bed resistance, friction losses in the chimney, sudden contraction or expansion, sudden bend in the flow, losses in the entry as well as the exit are considered while calculating the flow rate mathematically.

Table 7 Thermal efficiency for different firepowers

Sr. no.	Firepower, kW	η_{expt}	η_{model}	% Error
1.	2.202	37.87	35.19	7.09
2.	2.981	34.44	36.69	-6.54
3.	3.119	34.58	37.13	-7.39

3.2 Thermal efficiency

The value of thermal efficiency of mathematical model is validated with the experimental results of high-power hot start test. The experimental and model values are found to be in good agreement. The average deviation is estimated to be 7%. Table 7 shows the value of thermal efficiency for different firepowers. The average value of thermal efficiency is just above Tier 3 [65].

3.3 Exhaust

3.3.1 Carbon monoxide (CO emissions)

The output of the mathematical model is given as input for the computational model to understand the working of the

cookstove. Figure 11 shows the variation of CO emissions in parts per million (ppm) with the firepower. The average deviation of experimental and computational values is 9.09%, and also the values predicted by the computational model are on the higher sides, so it is safe to design cookstove with the help of a mathematical and computational model. The exhaust was also calculated by WBT standard in g/MJ_d . The average value of CO in g/MJ_d for high-power test was 10.59. Figure 12 shows the comparison of CO emissions for different stoves available in the literature [5, 29]. The stoves like Uganda 2-pot, Onil stove and Justa stove which are sunken pot stoves can have a good comparison with the present model. The advantage with the current design is that no specified pots are required for the operation of stove likewise in the other two-pot stoves mentioned above. The

Fig. 11 Variation of CO with firepower

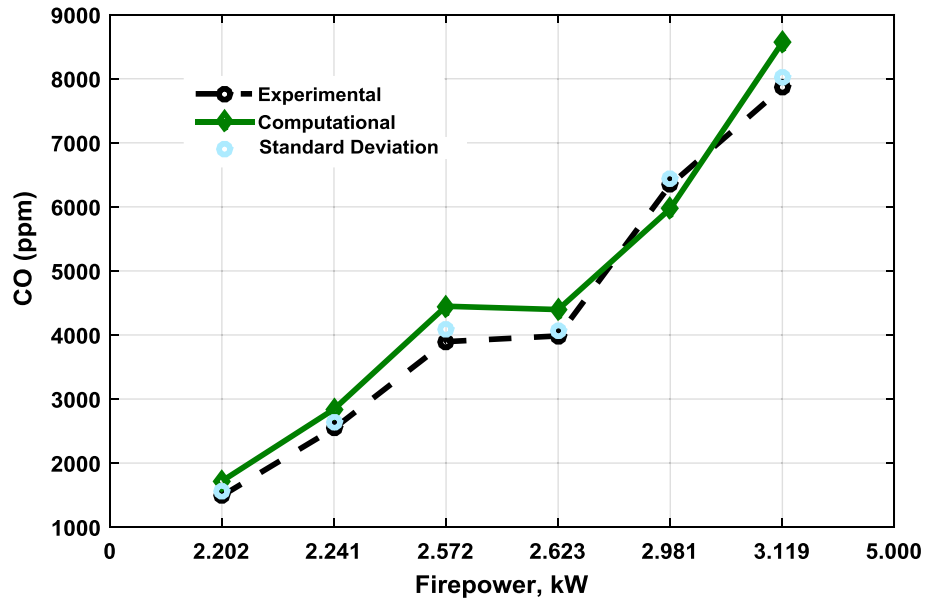
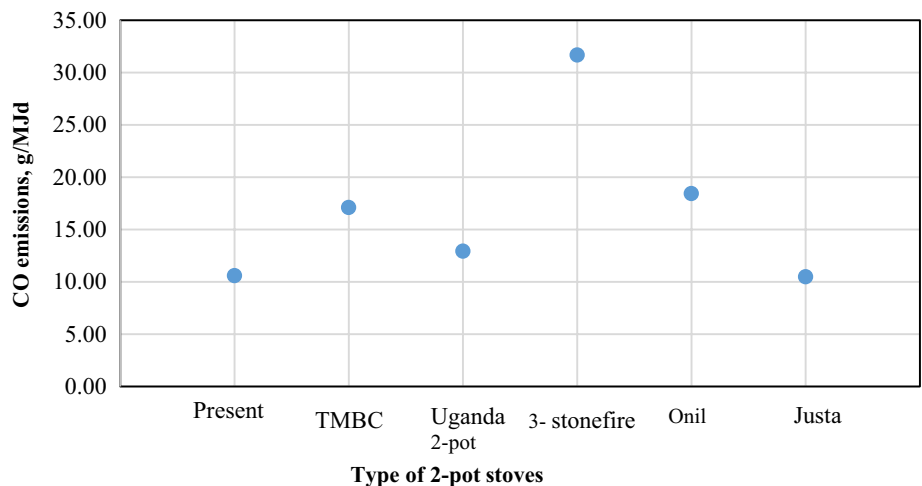


Fig. 12 Comparison of CO emissions with stoves available in the literature



values of CO are considerably low compared to traditional multipot biomass and 3 stone fire available on the field.

3.3.2 Combustion efficiency

The value of modified combustion is given as,

$$MCE = \frac{CO_2}{CO_2 + CO}$$

The variation of experimental and computational modified combustion efficiencies is shown in Table 8. The computational values are in good agreement with the experimental results.

The value of modified combustion efficiency decreases with increasing firepower; it means the combustion deteriorates as we increase the firepower keeping the same IAR [66]. The same is observed in the experimental as well as computational results.

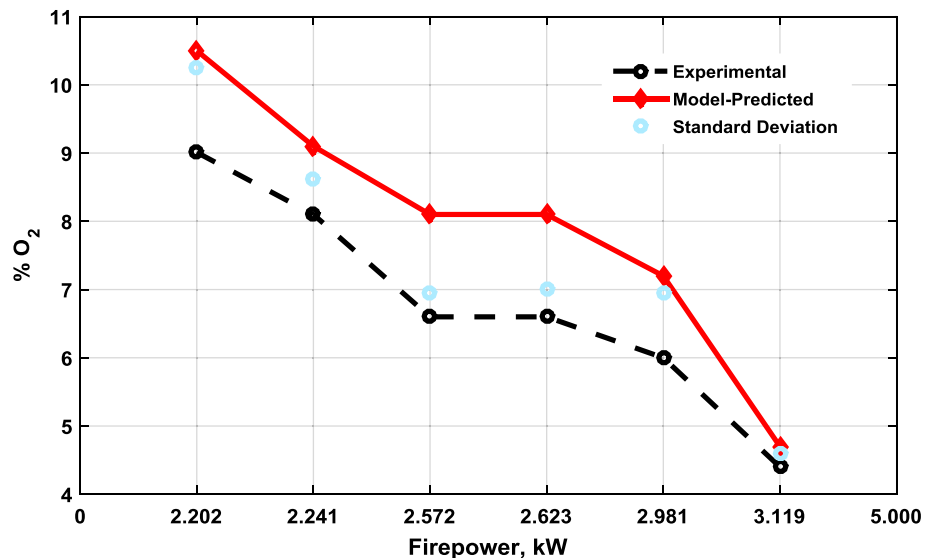
3.3.3 Percentage of O₂ variation

Variation of O₂% with firepower is shown in Fig. 13. The trend of O₂ is same as predicted by the other researchers [20,

Table 8 Variation of modified combustion efficiency with firepower

Firepower (kW)	MCE, experimental values (%)	MCE, computational values (%)	% Error
2.202	98.39	98.05	0.35
2.241	97.47	97.18	0.30
2.572	96.56	95.98	0.60
2.623	96.49	96.02	0.48
2.981	94.73	95.01	-0.30
3.119	94.14	93.89	-1.03

Fig. 13 Variation of O₂ with firepower



40]. The values of O₂% decrease with increase in firepower. As firepower is directly proportional to mass flow rate, after increasing the fuel input, the amount of air decreases, i.e. by inserting more sticks in the feeding zone, we restrict the flow of air into the combustion zone. The same is observed in the case of modelling as well as experimentation. The average variation of O₂% between experimental and computational values is 18%.

3.4 Flow structures

Figure 14a shows the temperature contours for different values of firepower. CFD helps in predicting the flow structure with the increase in the firepower. The flame propagation increases with the increase in firepower. The shifting of the higher-temperature zone can be seen through the temperature contours. Figure 14b shows the streamlines which help in detecting the flow pattern in the selected geometry, and also, it determines the wake region and gives a clear picture of the flow at the exit. The distribution of the flow at the bottom can be seen through the streamlines. Also, CFD helps in determining other parameters like velocity, concentration of species, etc.

4 Model limitations and future scope

The mathematical model is applied where the mass of flue remains constant throughout the working zone of the cookstove. Also, the model holds good only for the natural draft cookstove and is not applicable for a forced draft or gasifier stove. The limitation of exhaust value determination by the mathematical model is overcome by using the computational model. In future, the mathematical as well as the computational model can be used to obtain the results much closer to

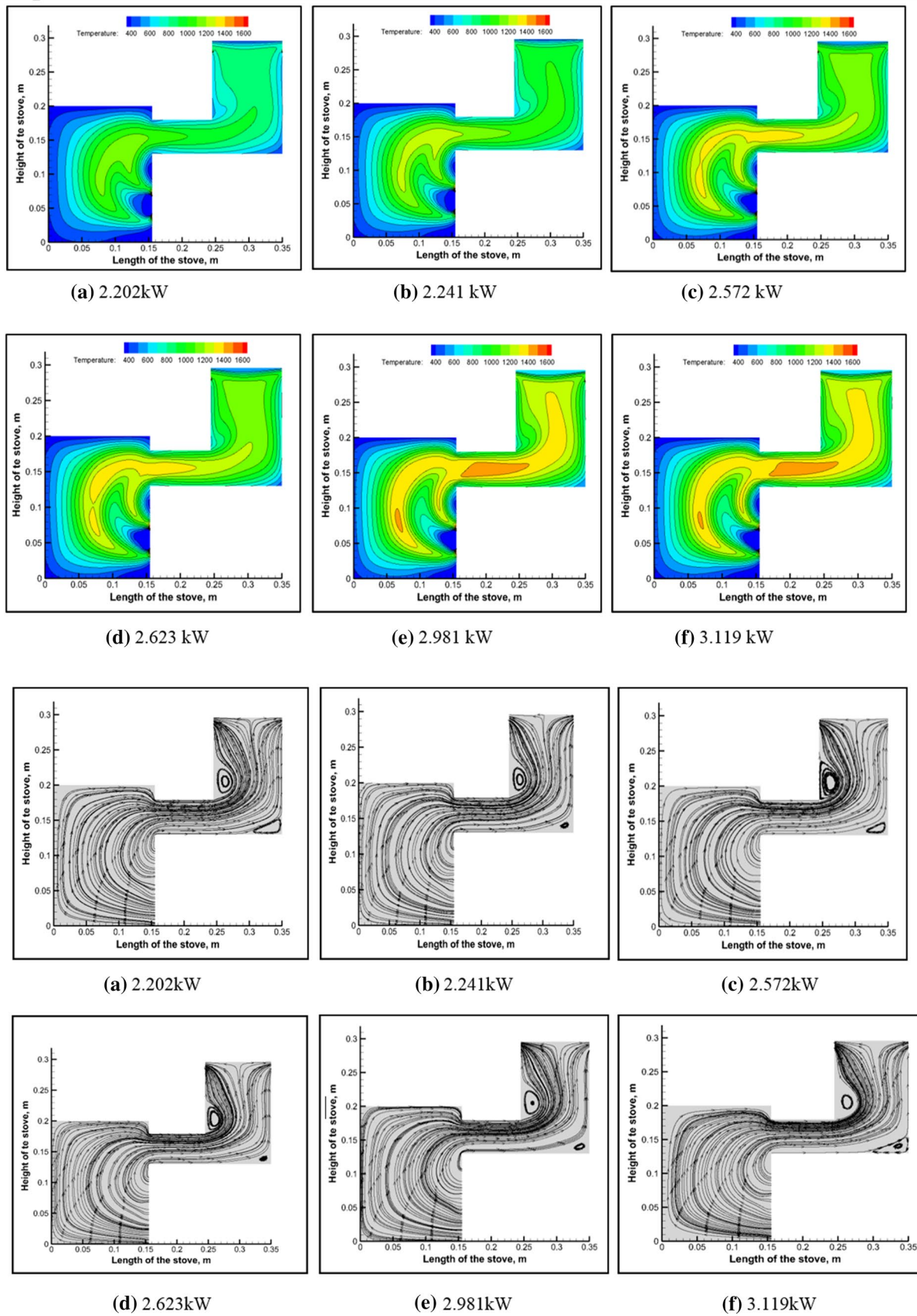


Fig. 14 a Temperature contours and b Flow streamlines for different firepowers

the experimental values. The model generates a large number of solutions for different geometrical and operational inputs. This will help to optimize the design, which is the task to be taken up in future.

5 Conclusions

The mathematical approach to design the cookstove serves to be a better solution to develop a new biomass cookstove. The model will help to predict the performance of cookstove for various geometrical inputs. The parameters like thermal efficiency, mass flow rates and flame temperatures at different locations can be predicted by the model. The non-premixed combustion model along with the PDF gives a better picture of the working of a cookstoves. This will not only save energy resources but will help in experimenting with different parameters of the cookstove. A detailed parametric analysis may result in finding a new parameter which may directly or indirectly affect the performance of cookstove. The model-predicted values of temperature, as well as exhaust, are varying with the maximum average deviation of 13 and 16%, respectively, from the experimental results. The cost of the instruments required to determine the values of CO and PM_{2.5} is too high and is not always available with the researcher. Hence, the combination of mathematical and computational modelling can be of great help to design cookstove with good accuracy.

Acknowledgments No external funds were provided by any institution.

References

- Rural Poverty Report (2011)
- Anhalt J, Holanda S (2009) Implementation of a dissemination strategy for efficient Cook Stoves in Northeast Brazil. Policy for Subsidizing Efficient Stoves
- Crewe E (1997) The silent traditions of developing cooks. In: Grillo R, Stirrat R (eds) Discourses of development: anthropological perspectives. Berg, Oxford
- Web of Science (2018). <http://apps.webofknowledge.com>. Accessed 6 Oct 2018
- Baldwin SF (1987) Biomass stove: engineering design, development, and dissemination. Center For Energy and Environmental Studies Princeton University, Princeton
- MacCarty N, Still OD (2010) Fuel use and emissions performance of fifty cooking stoves in the laboratory and related benchmark of performance. Elsevier, Amsterdam
- Kumar M, Kumar S, Tyagi SK (2013) Design, development and technological advancement in the biomass cookstoves: a review. *Renew Sustain Energy Rev* 26:265–285. <https://doi.org/10.1016/j.rser.2013.05.010>
- Kshirsagar MP, Kalamkar VR (2014) A comprehensive review on biomass cookstoves and a systematic approach for modern cookstove design. *Renew Sustain Energy Rev* 30:580–603
- Sutar KB, Kohli S, Ravi MR, Ray A (2015) Biomass cookstoves: a review of technical aspects. *Renew Sustain Energy Rev* 41:1128–1166. <https://doi.org/10.1016/j.rser.2014.09.003>
- Sedighi M, Salarian H (2017) A comprehensive review of technical aspects of biomass cookstoves. *Renew Sustain Energy Rev* 70:656–665. <https://doi.org/10.1016/j.rser.2016.11.175>
- Mehetre SA, Panwar NL, Sharma D, Kumar H (2017) Improved biomass cookstoves for sustainable development: a review. *Renew Sustain Energy Rev* 73:672–687
- Joseph S, Shanahan Y (1980) Designing a test procedure for domestic Woodburning Stoves. Microfich Ref Libr, Oxford
- Volunteers in Technical Assistance (1982) Testing the efficiency of wood-burning Cookstoves: provisional international standards. In: Proceedings of a meeting of experts at volunteers in technical assistance (VITA)
- Johnson M, Lam N, Brant S et al (2011) Modeling indoor air pollution from cookstove emissions in developing countries using a Monte Carlo single-box model. *Atmos Environ* 45:3237–3243. <https://doi.org/10.1016/j.atmosenv.2011.03.044>
- Singh S, Gupta GP, Kumar B, Kulshrestha UC (2014) Comparative study of indoor air pollution using traditional and improved cooking stoves in rural households of Northern India. *Energy Sustain Dev* 19:1–6. <https://doi.org/10.1016/j.esd.2014.01.007>
- Grabow K, Still D, Bentson S (2013) Test kitchen studies of indoor air pollution from biomass cookstoves. *Energy Sustain Dev* 17:458–462. <https://doi.org/10.1016/j.esd.2013.05.003>
- Singh A, Tuladhar B, Bajracharya K, Pillarisetti A (2012) Assessment of effectiveness of improved cook stoves in reducing indoor air pollution and improving health in Nepal. *Energy Sustain Dev* 16:406–414. <https://doi.org/10.1016/j.esd.2012.09.004>
- Agenbroad JN (2010) A simplified model for understanding Natural convection driven biomass cooking stoves. MS Thesis, Colorado State University. <https://doi.org/10.1017/cbo9781107415324.004>
- Agenbroad J, DeFoort M, Kirkpatrick A, Kreutzer C (2011) A simplified model for understanding natural convection driven biomass cookingstoves—part 1: with setup and baseline validation. *Energy Sustain Dev* 15:160–168
- Kshirsagar MP, Kalamkar VR (2015) A mathematical tool for predicting thermal performance of natural draft biomass cookstoves and identification of a new operational parameter. *Energy* 93:188–201
- Oanh NTK, Albina DO, Ping L, Wang X (2005) Emission of particulate matter and polycyclic aromatic hydrocarbons from select cookstove-fuel systems in Asia. *Biomass Bioenergy* 28:579–590. <https://doi.org/10.1016/j.biombioe.2005>
- Yuntenwi EAT, MacCarty N, Still D, Ertel J (2008) Laboratory study of the effects of moisture content on heat transfer and combustion efficiency of three biomass cook stoves. *Energy Sustain Dev* 12:66–77. [https://doi.org/10.1016/S0973-0826\(08\)60430-5](https://doi.org/10.1016/S0973-0826(08)60430-5)
- Shen G (2016) Changes from traditional solid fuels to clean household energies—opportunities in emission reduction of primary PM_{2.5} from residential cookstoves in China. *Biomass Bioenergy* 86:28–35. <https://doi.org/10.1016/j.biombioe.2016.01.004>
- Arora P, Jain S (2016) A review of chronological development in cookstove assessment methods: challenges and way forward. *Renew Sustain Energy Rev* 55:203–220. <https://doi.org/10.1016/j.rser.2015.10.142>
- Bhattacharya SC, Albina DO, Salam PA (2002) Emission factors of wood and charcoal-Fired cookstoves. *Biomass Bioenergy* 23:453–469
- Scott P (2005) Stove design and performance testing workshop. Public Health. WHO IAP Workshop Kampala, Uganda. 17 June
- Nazmul Alam SM, Chowdhury SJ (2010) Improved earthen stoves in coastal areas in Bangladesh: economic, ecological and

- socio-cultural evaluation. *Biomass Bioenergy* 34:1954–1960. <https://doi.org/10.1016/j.biombioe.2010.08.007>
28. Adkins E, Tyler E, Wang J et al (2010) Field testing and survey evaluation of household biomass cookstoves in rural sub-Saharan Africa. *Energy Sustain Dev* 14:172–185. <https://doi.org/10.1016/j.esd.2010.07.003>
 29. Pande RR, Kalamkar VR, Kshirsagar M (2018) Making the popular clean: improving the traditional multipot biomass cookstove in Maharashtra, India. *Environ Dev Sustain* 21:1391–1410. <https://doi.org/10.1007/s10668-018-0092-4>
 30. Honkalaskar VH, Bhandarkar UV, Sohoni M (2013) Development of a fuel efficient cookstove through a participatory bottom-up approach. *Energy Sustain Soc* 3:16
 31. Joshi M, Srivastava RK (2013) Development and performance evaluation of an improved three pot Cook Stove for cooking in rural Uttarakhand, India. *Int J Adv Res* 1(5):596–602
 32. MacCarty N, Still D, Ogle D (2010) Fuel use and emissions performance of fifty cooking stoves in the laboratory and related benchmarks of performance. *Energy Sustain Dev* 14(3):161–171
 33. Kshirsagar MP, Kalamkar VR (2016) User-centric approach for the design and sizing of natural convection biomass cookstoves for lower emissions. *Energy* 115(Part-I):1202–1215
 34. The India State-Level Disease Burden Initiative report (2017). phfi.org/the-work/research/the-india-state-level-disease-burden-initiative
 35. Test Results of Cook Stove Performance. Approvech Res Cent Shell Foundation, USA vol 1, pp 1–52
 36. Ochieng C, Vardoulakis S, Tonne C (2017) Household air pollution following replacement of traditional open fire with an improved rocket type cookstove. *Sci Total Environ* 580:440–447. <https://doi.org/10.1016/j.scitotenv.2016.10.233>
 37. WHO (2018) Household air pollution and health. www.who.int
 38. Poddar M, Chakrabarti S (2016) Indoor air pollution and women's health in India: an exploratory analysis. *Environ Dev Sustain* 18:669–677. <https://doi.org/10.1007/s10668-015-9670-x>
 39. Geremew K, Gedefaw M, Dagnev Z, Jara D (2014) Current level and correlates of traditional cooking energy sources utilization in urban settings in the context of climate change and health, North-west Ethiopia: a case of Debre Markos town. *Biomed Res Int*. <https://doi.org/10.1155/2014/572473>
 40. Samson R, Stohl D, Elepano A, De Maio A. Enhancing household biomass energy use in the Philippines. Excerpt from Chapter 2, pp 1–28
 41. Varunkumar S, Rajan NKS, Mukunda HS (2012) Experimental and computational studies on a gasifier based stove. *Energy Convers Manag* 53:135–141. <https://doi.org/10.1016/j.enconman.2011.08.022>
 42. Dasappa S, Paul PJ (2001) Gasification of char particles in packed beds: analysis and results. *Int J Energy Res* 25:1053–1072. <https://doi.org/10.1002/er.740>
 43. Sakonidou EP, Karapantsios TD, Balouktsis AI, Chassapis D (2008) Modeling of the optimum tilt of a solar chimney for maximum air flow. *Sol Energy* 82(1):80–94
 44. Ong KS, Chow CC (2003) Performance of a solar chimney. *Solar* 74(1):1–17
 45. Holman JP (2010) Heat transfer, 10th edn. Mc-Graw-Hill, New York
 46. Shah R, Date AW (2011) Steady-state thermo chemical model of a wood-burning cook-stove. *Combust Sci Technol* 183:321–346. <https://doi.org/10.1080/00102202.2010.516617>
 47. Kothandaraman CP (2006) Fundamentals of heat and mass transfer, 3rd edn
 48. Siegel R, Howell JR (1992) Thermal radiation heat transfer, 3rd edn. McGraw-Hill, New York
 49. Prasad KK, Bussmann P, Visser P, Delsing J, Claus J, Sulilatu W (1981) Some studies on open fires, shielded fires and heavy stoves. A report, the wood burning stove group. Departments of Applied Physics and Mechanical Engineering, Eindhoven University of Technology and Division of Technology for Society, TNO, Apeldoorn
 50. Liu K, Han W, Pan WP, Riley JT (2001) Polycyclic aromatic hydrocarbon (PAH) emissions from a coal-fired pilot FBC system. *J Hazard Mater* 84:175–188. [https://doi.org/10.1016/S0304-3894\(01\)00196-0](https://doi.org/10.1016/S0304-3894(01)00196-0)
 51. Hayes S, Bateman P (2002) English handbook for Wood Pellet combustion English handbook for Wood Pellet combustion. Technology, pp 1–86
 52. Carvalho L, Wopienka E, Pointner C (2013) Performance of a pellet boiler fired with agricultural fuels. *Appl Energy* 104:286–296. <https://doi.org/10.1016/j.apenergy.2012.10.058>
 53. Obaidullah M, Dyakov IV, Thomassin JD et al (2014) CO emission measurements and performance analysis of 10 kW and 20 kW wood stoves. *Energy Proc* 61:2301–2306. <https://doi.org/10.1016/j.egypro.2014.12.443>
 54. Obernberger I, Brunner T, Mandl C et al (2017) Strategies and technologies towards zero emission biomass combustion by primary measures. *Energy Proc* 120:681–688. <https://doi.org/10.1016/j.egypro.2017.07.184>
 55. Kraszkiewicz A, Przywara A, Kachel-Jakubowska M, Lorencowicz E (2015) Combustion of plant biomass pellets on the grate of a low power boiler. *Agric Agric Sci Proc* 7:131–138. <https://doi.org/10.1016/j.aaspro.2015.12.007>
 56. Sun J, Shen Z, Zhang L et al (2018) Impact of primary and secondary air supply intensity in stove on emissions of size-segregated particulate matter and carbonaceous aerosols from apple tree wood burning. *Atmos Res* 202:33–39. <https://doi.org/10.1016/j.atmosres.2017.11.010>
 57. Bhandari S, Gopi S, Date A (1988) Investigation of CTARA wood-burning stove. Part I. Experimental investigation. *Sadhana* 13:271–293. <https://doi.org/10.1007/BF02759889>
 58. Bussmann PJT, Visser P, Prasad KK (1983) Open fires: experiments and theory. *Proc Indian Acad Sci Sect C Eng Sci* 6:1–34. <https://doi.org/10.1007/BF02843288>
 59. Slipper B, Nottingham T, User NE, Burnham-Slipper, Hugh (2009) Breeding a better stove: the use of computational fluid dynamics and genetic algorithms to optimise a wood burning stove for Eritrea. PhD thesis, University of Nottingham
 60. Ravi MR, Kohli S, Ray A (2002) Use of CFD simulation as a design tool for biomass stoves. *Energy Sustain Dev* 6:20–27. [https://doi.org/10.1016/S0973-0826\(08\)60309-9](https://doi.org/10.1016/S0973-0826(08)60309-9)
 61. Gupta R, Mittal ND (2010) Fluid flow and heat transfer in a single-pan wood stove. *Int J Eng Sci* 2:4312–4324
 62. Chaney J, Liu H, Li J (2012) An overview of CFD modelling of small-scale fixed-bed biomass pellet boilers with preliminary results from a simplified approach. *Energy Convers Manag* 63:149–156. <https://doi.org/10.1016/j.enconman.2012.01.036>
 63. Biswas G, Eswaran V (2002) Turbulent flows-fundamentals, experiments and modeling. Alpha Science International Ltd, Oxford
 64. Persson T, Fiedler F, Nordlander S et al (2009) Validation of a dynamic model for wood pellet boilers and stoves. *Appl Energy* 86:645–656. <https://doi.org/10.1016/j.apenergy.2008.07.004>
 65. International Organization for Standardization (2012) IWA 11: 2012 Guidelines for evaluating cookstove performance
 66. Pande RR, Kshirsagar MP, Kalamkar VR (2018) Experimental and CFD analysis to study the effect of inlet area ratio in a natural draft biomass cookstove. *Environ Dev Sustain*. <https://doi.org/10.1007/s10668-018-0269-x>

Publisher's Note Springer Nature remains neutral with regard to jurisdictional claims in published maps and institutional affiliations.